A Class of Continuous Predefined-Time Controllers

Esteban Jiménez-Rodríguez, *Dept. of Electrical Engineering, Cinvestav - Guadalajara*, Zapopan, México, ejimenezr@gdl.cinvestav.mx

Aldo J. Muñoz-Vázquez, *CONACYT Research Fellow, School of Enginering, UACH*, Chihuahua, México, aldo.munoz.vazquez@gmail.com

Juan Diego Sánchez-Torres, *Dept. of Math. and Phys., ITESO*, Tlaquepaque, México, dsanchez@iteso.mx

Alexander G. Loukianov, *Dept. of Electrical Engineering, Cinvestav - Guadalajara*, Zapopan, México, louk@gdl.cinvestav.mx

***Abstract*—A class of continuous predefined-time controllers is designed in this paper. The control structure is built upon a class of comparison functions, whose features allow to analyze the predefined-time convergence property in the Lyapunov framework. Rather than providing exact predefined-time convergence to the equilibrium point, the proposed controller guarantees *uniform predefined-time ultimate predefined boundedness* of the solutions, i.e., the capability of setting an arbitrarily desired ultimate bound and an arbitrarily desired convergence time, through an appropriate selection of the controller parameters. Moreover, for a class of second-order systems, an additional analysis is carried out to show finite-gain input-output stability. The reliability of the proposed scheme is highlighted through numerical simulations in a representative example.**

***Index Terms*—Predefined-time convergence; Lyapunov-based methods; Robust control; Sliding-mode control**

I. Introduction

Several industrial applications like batch processes control and monitoring, faults isolation, among others, demand the satisfaction of time-response constraints to satisfy safety, regulatory or quality standards. To cope with this time-response requirements, the notion of *finite-time stability* has attracted a lot of attention during the last 50 years [1]–[4]. On the same line, the recent *fixed-time stability* concept, which is a stronger form of finite-time stability since it allows to eliminate the lack of boundedness of the settling-time function, has given solution to some sophisticated control problems [5]–[8].

Even though fixed-time stability is per se a significant conceptual advantage over finite-time stability for some applications, in turn, it presents the difficulty that is not straightforward to tune the system parameters to achieve a desired fixed time. To overcome this drawback, a class of dynamical systems that exhibit the property of *predefined-time stability* has been studied within the last six years [9].

Predefined-time stability is a promising and useful property, which brings advanced stability features to the closed-loop system response, such that, after an arbitrary user-prescribed time, the system state is stabilized, providing a high degree of certainty on the system behaviour. Due to its exciting features, several predefined-time control schemes have been developed for first-order systems [9], [10], for second-order systems [11], [12], for systems subject to nonholonomic constraints [13], for robotic manipulators [14], [15], among others.

All the mentioned works on predefined-time controller design make use of discontinuous high-frequency control terms to deal with nonvanishing disturbances and guaranteeing predefined-time exact convergence to the equilibrium point. However, such discontinuous control terms might deteriorate the components of a real physical system due to high-frequency oscillations, or might even be impossible to implement due to a limited actuator response. In this scenario, one may opt for sacrificing the exact convergence in order to obtain a continuous controller.

In this sense, this paper is devoted to the design of continuous predefined-time controllers which guarantee the *uniform predefined-time ultimate predefined boundedness* of the solutions, i.e., the capability of setting an arbitrarily desired ultimate bound and an arbitrarily desired convergence time, through an appropriate selection of the controller parameters. The control structure is built upon a novel class of comparison function, whose features allow to analyze the predefined-time convergence property in the Lyapunov framework. Moreover, for a class of second-order systems, an additional analysis is carried out to show finite-gain input-output stability. The behaviour of the proposed class of controllers is illustrated through a representative numerical simulation example of a two-link planar manipulator.

II. Preliminaries

A. Notation

We use the following notation throughout the paper: $\mathbb{R}$ stands for the set of real numbers; moreover $\mathbb{R}_+ = \{x \in \mathbb{R} : x > 0\}$, $\mathbb{R}_{\geq 0} = \{x \in \mathbb{R} : x \geq 0\}$ and $\bar{\mathbb{R}}_+ = \mathbb{R}_+ \cup \{\infty\}$. For $\boldsymbol{x} \in \mathbb{R}^n$, $\boldsymbol{x}^T$ denotes its transpose, $||\boldsymbol{x}|| = \sqrt{\boldsymbol{x}^T\boldsymbol{x}}$ its norm, and $B_r(\boldsymbol{x}) = \{\boldsymbol{y} \in \mathbb{R}^n : ||\boldsymbol{y} - \boldsymbol{x}|| < r\}$ its $r-$vicinity. The function $x \to \lfloor x \rceil^h$ is defined as $\lfloor x \rceil = |x|^h \text{sign}(x)$ for any $x \in \mathbb{R}$ if $h > 0$, and for any $x \in \mathbb{R} \setminus \{0\}$ if $h \leq 0$. $\theta'(z) = \frac{d\theta}{dz}$ denotes the first derivative of the function $\theta : \mathbb{R} \to \mathbb{R}$.

B. A vector power function and some properties

The following is a vector extension of the *odd power function* $\lfloor x \rceil^h$.

Definition 1 ([12]). Let $h \geq 0$. For $\boldsymbol{x} \in \mathbb{R}^n \setminus \{\boldsymbol{0}\}$, define the function

$$||\lfloor \boldsymbol{x} \rceil||^h = \frac{\boldsymbol{x}}{||\boldsymbol{x}||^{1-h}}.$$

Since $\lim_{\boldsymbol{x}\to 0} ||\lfloor \boldsymbol{x} \rceil||^h = \boldsymbol{0}$ for $h > 0$, it is considered that $||\lfloor \boldsymbol{0} \rceil||^h = \boldsymbol{0}$. Therefore, the function $||\lfloor \boldsymbol{x} \rceil||^h$ is continuous for $0 < h < 1$ and discontinuous in $\boldsymbol{x} = \boldsymbol{0}$ for $h = 0$.

Proposition 1 ([12]). *Let $\epsilon > 0$. The continuous approximation of the unit vector complies to:*

(i) $\frac{\boldsymbol{x}}{||\boldsymbol{x}||+\epsilon} = \lfloor\lfloor \boldsymbol{x} \rceil\rceil^0 - \frac{\epsilon\lfloor\lfloor \boldsymbol{x} \rceil\rceil^0}{||\boldsymbol{x}||+\epsilon}$.

For $h > 0$, the function $\lfloor\lfloor \boldsymbol{x} \rceil\rceil^h$ fulfills:

(ii) $\lfloor\lfloor -\boldsymbol{x} \rceil\rceil^h = -\lfloor\lfloor \boldsymbol{x} \rceil\rceil^h$;

(iii) $\lfloor\lfloor \boldsymbol{x} \rceil\rceil^0 = \frac{\boldsymbol{x}}{||\boldsymbol{x}||}$, *for* $\boldsymbol{x} \neq \mathbf{0}$;

(iv) $\lfloor\lfloor \boldsymbol{x} \rceil\rceil^1 = \lfloor\lfloor \boldsymbol{x} \rceil\rceil = \boldsymbol{x}$.

Furthermore, for $h_1, h_2 \in \mathbb{R}$, it follows:

(v) $\lfloor\lfloor \boldsymbol{x} \rceil\rceil^{h_1} ||\boldsymbol{x}||^{h_2} = ||\boldsymbol{x}||^{h_1} \lfloor\lfloor \boldsymbol{x} \rceil\rceil^{h_2} = \lfloor\lfloor \boldsymbol{x} \rceil\rceil^{h_1+h_2}$, *and*

(vi) $\lfloor\lfloor \boldsymbol{x}^T \rceil\rceil^{h_1} \lfloor\lfloor \boldsymbol{x} \rceil\rceil^{h_2} = ||\boldsymbol{x}||^{h_1+h_2}$.

C. On predefined-time ultimate boundedness

Consider the following system:

$$\dot{\boldsymbol{x}} = \boldsymbol{f}(t, \boldsymbol{x}; \boldsymbol{\rho}), \quad \boldsymbol{x}(t_0) = \boldsymbol{x}_0, \quad t_0 \in \mathbb{R}_{\geq 0} \tag{1}$$

where $\boldsymbol{x} \in \mathbb{R}^n$ is the system state, the vector $\boldsymbol{\rho} \in \mathbb{R}^l$ stands for the *tunable* parameters of (1). The function $\boldsymbol{f} : \mathbb{R}_{\geq 0} \times \mathbb{R}^n \to \mathbb{R}^n$ is continuous, and such that the solutions of (1) exist and are unique. Thus, $\boldsymbol{\Phi}(t, \boldsymbol{x}_0, t_0)$ denotes the solution of (1) starting from $\boldsymbol{x}_0 \in \mathbb{R}^n$ at $t = t_0$.

Remark 1. Working with parametrized system (1) means we consider a control system

$$\dot{\boldsymbol{x}} = \boldsymbol{g}(t, \boldsymbol{x}, \boldsymbol{u}), \tag{2}$$

where the input $\boldsymbol{u} \in \mathbb{R}^m$ is specified as a feedback function of the state $\boldsymbol{x}$ with tunable control parameters $\boldsymbol{\rho}$, i.e., $\boldsymbol{u} = \boldsymbol{\phi}(\boldsymbol{x}; \boldsymbol{\rho})$, with $\boldsymbol{\phi} : \mathbb{R}^n \to \mathbb{R}^m$. Replacing $\boldsymbol{u} = \boldsymbol{\phi}(\boldsymbol{x}; \boldsymbol{\rho})$ in (2) eliminates $\boldsymbol{u}$ and yields the parametrized autonomous dynamics (1), with $\boldsymbol{f}(t, \boldsymbol{x}; \boldsymbol{\rho}) := \boldsymbol{g}(t, \boldsymbol{x}, \boldsymbol{\phi}(\boldsymbol{x}; \boldsymbol{\rho}))$.

When dealing with systems subject to nonvanishing perturbations, we do not know if the origin is an equilibrium point of (1) (i.e., if $\boldsymbol{f}(t, \mathbf{0}; \boldsymbol{\rho}) = 0$). Hence, we cannot study the stability of the origin as an equilibrium point of (1). Instead, we may expect that if the perturbations are "small", the solutions of (1) will also be "small" eventually. This notion is formally defined below.

Definition 2 (Uniform ultimate boundedness [16]). The solutions of (1) are said to be **uniformly ultimately bounded** if there exists $b_0 \in \mathbb{R}_+$, and for every $a \in \mathbb{R}_+$ there is some $T = T(a)$ such that

$$||\boldsymbol{x}_0|| < a \Rightarrow ||\boldsymbol{\Phi}(t, \boldsymbol{x}_0, t_0)|| \leq b_0, \quad \forall, t \geq t_0 + T.$$

Example 1 ([16]). Consider the scalar system

$$\dot{x} = -x + \delta \sin t, \quad x(t_0) = a, \quad a > \delta > 0,$$

where $x \in \mathbb{R}$ is the system state. One can easily see that this system does not have any equilibrium points.

Moreover, if one takes some $b_0 \in (\delta, a)$, it can be shown (see [16]) that

$$|\Phi(t, a, t_0)| \leq b_0, \quad \forall t \geq t_0 + T(a)$$

where $T(a) = \ln \frac{a-\delta}{b_0-\delta}$. This is, the solutions are uniformly ultimately bounded.

Having Definition 2 and Example 1 at hand, some issues can be noticed:

- in general, the bound b_0 of the solutions is implicitly restricted by the bound of the perturbation terms;
- often, the time $T(a)$ grows with no upper bound as the number a, which is related with the norm of the initial condition, grows.

On the other hand, from a controller designer point of view, it would be desirable to be able to:

(i) assign an *arbitrary* bound b to the solutions of the system, and

(ii) set an *arbitrary* upper bound T_c for the time when the solutions must enter to the region bounded by b;

all of this through an appropriate selection of the tunable parameters $\boldsymbol{\rho}$ of system (1).

Hence, to distinguish the case when the desirable properties *(i)* and *(ii)* are met, the notion of *uniform predefined-time ultimate predefined boundedness* is formally defined below.

Definition 3 (Uniform predefined-time ultimate predefined boundedness (UPTUPB)). The solutions of (1) is said to be **uniformly predefined-time ultimately bounded with predefined bound** if for any $T_c, b \in \mathbb{R}_+$, there exists some $\boldsymbol{\rho} = \boldsymbol{\rho}(T_c, b) \in \mathbb{R}^l$ such that

$$||\boldsymbol{\Phi}(t, \boldsymbol{x}_0, t_0)|| \leq b, \quad \forall t \geq t_0 + T_c,$$

for any $\boldsymbol{x}_0 \in \mathbb{R}^n$.

D. Class $\mathcal{K}^1$ and class $\mathcal{W}$ functions

Inspired in the class-$\mathcal{K}$ functions in [17, Definition 1] and [16, Definition 4.2], the class-$\mathcal{K}^1$ functions are defined as follows:

Definition 4 ($\mathcal{K}^1$ functions). A scalar continuous function $\kappa : \mathbb{R}_{\geq 0} \to [0, 1)$ is said to belong to class $\mathcal{K}^1$, denoted as $\kappa \in \mathcal{K}^1$, if it is strictly increasing, $\kappa(0) = 0$ and $\kappa(r) \to 1$ as $r \to \infty$.

Remark 2 (Invertibility of $\mathcal{K}^1$ functions). $\mathcal{K}^1$ functions are bijective. In fact, let $\kappa \in \mathcal{K}^1$:

- it is injective (one-to-one) because it is continuous and strictly increasing;
- its image is $\kappa(\mathbb{R}_{\geq 0}) = [0, 1)$, thus it is surjective (onto).

Thus, since every class $\mathcal{K}^1$ function is bijective, their inverses exist. Moreover, since $\mathcal{K}^1$ functions are increasing, they are homeomorphisms.

The next lemma states some useful properties of class-$\mathcal{K}_\infty$ and class-$\mathcal{K}^1$ functions, which will be used in the next section.

Lemma 1. *Let $\alpha \in \mathcal{K}_\infty$ (see [17, Definition 1]) and $\kappa_1, \kappa_2 \in \mathcal{K}^1$. Then, $\kappa_1 \circ \alpha \in \mathcal{K}^1$, and $\kappa_1^{-1} \circ \kappa_2 \in \mathcal{K}_\infty$.*

Proof. The composition of increasing functions is increasing. Moreover, note that $(\kappa_1 \circ \alpha)(0) = \kappa_1(\alpha(0)) = \kappa_1(0) = 0$ and $(\kappa_1^{-1} \circ \kappa_2)(0) = \kappa_1^{-1}(\kappa_2(0)) = \kappa_1^{-1}(0) = 0$. Finally, since κ_1 is an homeomorphism,

$$\lim_{r\to\infty} (\kappa_1 \circ \alpha)(r) = \kappa_1 \left(\lim_{r\to\infty} \alpha(r) \right) = 1,$$

and

$$\lim_{r\to\infty}(\kappa_1^{-1}\circ\kappa_2)(r)=\kappa_1^{-1}\left(\lim_{r\to\infty}\kappa_2(r)\right)=\infty.$$

□

Often, control design tasks require functions to meet certain properties like continuity, differentiability or some smoothness property. In this sense, class $\mathcal{W}\subset\mathcal{K}^1$ are defined as follows:

Definition 5. A scalar continuous function $\omega:\mathbb{R}_{\geq 0}\to[0,1)$ is said to belong to class $\mathcal{W}$, denoted as $\omega\in\mathcal{W}$, if $\omega\in\mathcal{K}^1$ is differentiable in $\mathbb{R}_+$, $\omega'(r)>0$ for $r>0$ and $\omega'(0)\in\bar{\mathbb{R}}_+$.

Example 2. Let $0<q<1$. Some examples of class $\mathcal{W}$ functions are:

(i) $\omega(r)=1-\exp(-r^q)$;
(ii) $\omega(r)=\frac{2}{\pi}\arctan(r^q)$; and
(iii) $\omega(r)=\frac{r^q}{r^q+\alpha}$, with $\alpha>0$.

III. Lyapunov Analysis for UPTUPB

Lyapunov analysis can be used to show UPTUPB of the solutions of (1), even if there is no equilibrium point at the origin. Sufficient conditions are stated in the following theorem:

Theorem 1. *Let $V:\mathbb{R}^n\to\mathbb{R}_{\geq 0}$ be a continuous, positive definite and radially unbounded function and $\omega\in\mathcal{W}$. If for any $T_c,\mu\in\mathbb{R}_+$, there exists some $\boldsymbol{\rho}\in\mathbb{R}^l$, such that the time-derivative of V along the trajectories of (1) satisfies*

$$\dot{V}(\boldsymbol{x})\leq-\frac{1}{T_c}\frac{1}{\omega'(V(\boldsymbol{x}))},\quad \textit{for}\ ||\boldsymbol{x}||\geq\mu, \tag{3}$$

then, for any $\boldsymbol{x}_0\in\mathbb{R}^n$ the solution $\boldsymbol{\Phi}(t,\boldsymbol{x}_0,t_0)$ of (1) satisfies

$$||\boldsymbol{\Phi}(t,\boldsymbol{x}_0,t_0)||\leq b=\kappa_1^{-1}(\kappa_2(\mu)),\quad \forall t\geq t_0+T_c,$$

where $\kappa_1,\kappa_2\in\mathcal{K}^1$. This is, the solutions of (1) are uniformly predefined-time ultimately bounded with predefined bound.

Moreover, if $V(\boldsymbol{x})=\alpha(||\boldsymbol{x}||)$, with $\alpha\in\mathcal{K}_\infty$, then $b=\mu$ in the above inequality.

Proof. Let $T_c,\mu\in\mathbb{R}_+$. Then, there exists $\boldsymbol{\rho}\in\mathbb{R}^l$ such that (3) holds. Since V is continuous, positive definite and radially unbounded, there exist $\alpha_1,\alpha_2\in\mathcal{K}_\infty$ such that [16, Lemma 4.3]:

$$\alpha_1(||\boldsymbol{x}||)\leq V(\boldsymbol{x})\leq\alpha_2(||\boldsymbol{x}||). \tag{4}$$

Now, consider the function $W(\boldsymbol{x})=\omega(V(\boldsymbol{x}))$. From (3), the time-derivative of W along the trajectories of (1) satisfies

$$\dot{W}(\boldsymbol{x})\leq-\frac{1}{T_c},\quad \text{for}\ ||\boldsymbol{x}||\geq\mu. \tag{5}$$

On the other hand, from (4), the function W satisfies $\kappa_1(||\boldsymbol{x}||)\leq W(\boldsymbol{x})\leq\kappa_2(||\boldsymbol{x}||)$, where $\kappa_i=\omega\circ\alpha_i\in\mathcal{K}^1$ for $i=1,2$ (see Lemma 1).

Note that $||\boldsymbol{x}||<\mu\iff\kappa_2(||\boldsymbol{x}||)<\kappa_2(\mu)\Rightarrow W(\boldsymbol{x})<\kappa_2(\mu)$, i.e. the set $\{\boldsymbol{x}\in\mathbb{R}^n:||\boldsymbol{x}||<\mu\}\subseteq\{\boldsymbol{x}\in\mathbb{R}^n:W(\boldsymbol{x})<\kappa_2(\mu)\}$, or equivalently $\{\boldsymbol{x}\in\mathbb{R}^n:W(\boldsymbol{x})\geq\kappa_2(\mu)\}\subseteq\{\boldsymbol{x}\in\mathbb{R}^n:||\boldsymbol{x}||\geq\mu\}$. Hence, inequality (5) holds for $W(\boldsymbol{x})\geq\kappa_2(\mu)$. This implies that the set $\{\boldsymbol{x}\in\mathbb{R}^n:W(\boldsymbol{x})\leq\kappa_2(\mu)\}$ is positively invariant, since the derivative $\dot{W}(\boldsymbol{x})$ is negative in its boundary $\{\boldsymbol{x}\in\mathbb{R}^n:W(\boldsymbol{x})=\kappa_2(\mu)\}$.

Now, we show that all trajectories starting in the set $\{\boldsymbol{x}\in\mathbb{R}^n:W(\boldsymbol{x})\geq\kappa_2(\mu)\}$, must enter the set $\{\boldsymbol{x}\in\mathbb{R}^n:W(\boldsymbol{x})\leq\kappa_2(\mu)\}$ within at most T_c time units. Let $\boldsymbol{\Phi}(t,\boldsymbol{x}_0,t_0)$, with $\boldsymbol{x}_0\in\{\boldsymbol{x}\in\mathbb{R}^n:W(\boldsymbol{x})\geq\kappa_2(\mu)\}$, be a solution of (1). From (5) and using the comparison lemma [16], it follows that

$$W(\boldsymbol{\Phi}(t,\boldsymbol{x}_0,t_0))\leq W(\boldsymbol{x}_0)-\frac{t-t_0}{T_c},$$

for $t\in[t_0,t_0+T_c(W(\boldsymbol{x}_0)-\kappa_2(\mu))]$. Hence, $W(\boldsymbol{\Phi}(t,\boldsymbol{x}_0,t_0))\leq\kappa_2(\mu)$ for all $t\geq t_0+T_c(W(\boldsymbol{x}_0)-\kappa_2(\mu))$, and consequently for all $t\geq T_c$.

Furthermore, note that $W(\boldsymbol{x})\leq\kappa_2(\mu)\Rightarrow\kappa_1(||\boldsymbol{x}||)\leq\kappa_2(\mu)\iff||\boldsymbol{x}||<\kappa_1^{-1}(\kappa_2(\mu))$. Hence, $||\boldsymbol{\Phi}(t,\boldsymbol{x}_0,t_0)||\leq\kappa_1^{-1}(\kappa_2(\mu)),\quad\forall t\geq t_0+T_c$.

Moreover, if $V(\boldsymbol{x})=\alpha(||\boldsymbol{x}||)$, then $\alpha_1=\alpha_2=\alpha$, and $\kappa_1=\kappa_2=\omega$, and the result follows. □

Theorem 1 is of paramount importance since it allows to analyze and show the UPTUPB property without the need of finding the explicit solution. Moreover, it will be very useful for designing a class of continuous predefined-time controllers in the next section.

IV. Continuous Predefined-Time Controllers

A. Problem statement

Consider the following affine control system:

$$\dot{\boldsymbol{y}}=\boldsymbol{g}(t,\boldsymbol{y})+\boldsymbol{B}(t,\boldsymbol{y})\left(\boldsymbol{u}+\boldsymbol{\delta}(t,\boldsymbol{y})\right),\quad \boldsymbol{y}(t_0)=\boldsymbol{y}_0, \tag{6}$$

where $\boldsymbol{y}\in\mathbb{R}^n$ is the system state, $\boldsymbol{u}\in\mathbb{R}^m$ is the control input, $\boldsymbol{\delta}:\mathbb{R}_{\geq 0}\times\mathbb{R}^n\to\mathbb{R}^n$ is a matched disturbance vector that includes plant parameter variations and external unknown perturbations, and the functions $\boldsymbol{g}:\mathbb{R}_{\geq 0}\times\mathbb{R}^n\to\mathbb{R}^n$ and $\boldsymbol{B}:\mathbb{R}_{\geq 0}\times\mathbb{R}^n\to\mathbb{R}^{n\times m}$ are continuous and such that $\operatorname{rank}\boldsymbol{B}(t,\boldsymbol{y})=m$ for all $(t,\boldsymbol{y})\in\mathbb{R}_{\geq 0}\times\mathbb{R}^n$.

Objective (O): to design a control input $\boldsymbol{u}$ such that the closed-loop solutions of (6) reach a vicinity with arbitrary desired radius $b\in\mathbb{R}_+$ of the manifold

$$\boldsymbol{x}(t,\boldsymbol{y})=0, \tag{7}$$

in an arbitrarily selected time $T_c\in\mathbb{R}_+$ and remain there for all $t\geq T_c$. The mapping $\boldsymbol{x}:\mathbb{R}_{\geq 0}\times\mathbb{R}^n\to\mathbb{R}^m$ in (7) is assumed to be smooth.

To meet objective **(O)**, consider the time derivative of $\boldsymbol{x}(t,\boldsymbol{y})$:

$$\dot{\boldsymbol{x}}=\boldsymbol{\sigma}(t,\boldsymbol{y})\boldsymbol{g}(t,\boldsymbol{y})+\boldsymbol{\sigma}(t,\boldsymbol{y})\boldsymbol{B}(t,\boldsymbol{y})\left(\boldsymbol{u}+\boldsymbol{\delta}(t,\boldsymbol{y})\right)+\frac{\partial\boldsymbol{x}(t,\boldsymbol{y})}{\partial t}, \tag{8}$$

where $\boldsymbol{\sigma}(t,\boldsymbol{y})=\frac{\partial\boldsymbol{x}(t,\boldsymbol{y})}{\partial\boldsymbol{y}}$. Then, assuming that $\boldsymbol{x}(t,\boldsymbol{y})$ is selected such that $\operatorname{rank}[\boldsymbol{\sigma}(t,\boldsymbol{y})\boldsymbol{B}(t,\boldsymbol{y})]=m$, for all $(t,\boldsymbol{y})\in\mathbb{R}_{\geq 0}\times\mathbb{R}^n$, the control input $\boldsymbol{u}$ can be chosen as

$$\boldsymbol{u}=-[\boldsymbol{\sigma}(t,\boldsymbol{y})\boldsymbol{B}(t,\boldsymbol{y})]^{-1}\left[\boldsymbol{\sigma}(t,\boldsymbol{y})\boldsymbol{g}(t,\boldsymbol{y})+\frac{\partial\boldsymbol{x}(t,\boldsymbol{y})}{\partial t}-\boldsymbol{v}\right], \tag{9}$$

where $\boldsymbol{v} \in \mathbb{R}^m$ is a virtual control input to be designed.

Substituting (9) in (8), results in

$$\dot{\boldsymbol{x}} = \boldsymbol{v} + \boldsymbol{\Delta}(t, \boldsymbol{y}), \quad \boldsymbol{x}(t_0, \boldsymbol{y}_0) = \boldsymbol{x}_0, \tag{10}$$

where $\boldsymbol{\Delta}(t, \boldsymbol{y}) = \boldsymbol{\sigma}(t, \boldsymbol{y})\boldsymbol{B}(t, \boldsymbol{y})\boldsymbol{\delta}(t, \boldsymbol{y})$, is assumed to be such that $||\boldsymbol{\Delta}(t, \boldsymbol{y})|| \leq \delta_0 + \delta_1 ||\boldsymbol{x}||^p$, with $\delta_0, \delta_1 \in \mathbb{R}_{\geq 0}$ and $p \in \mathbb{R}_+$ are known constants.

Remark 3. In the following, $\boldsymbol{\Phi}_y(t, \boldsymbol{y_0}, t_0)$ will make reference to a solution of system (6), whereas $\boldsymbol{\Phi}_x(t, \boldsymbol{y_0}, t_0)$ will make reference to a solution of system (10). We include indices x and y to avoid a possible confusion, since we will be working with either sytems (6) and (10) and their solutions.

After the above analysis, objective **(O)** can be re-stated formally as: to design a virtual control input $\boldsymbol{v}$ such that the solutions of (10) satisfy the UPTUPB property.

B. Proposed solution

The design of the virtual control input $\boldsymbol{v}$ is summarized in the following theorem:

Theorem 2. *Consider system* (10). *If the virtual control input is selected as*

$$\boldsymbol{v} = -\frac{1}{\rho_1} \frac{||\lfloor \boldsymbol{x} \rceil||^0}{\omega'(||\boldsymbol{x}||)} - \rho_2 \frac{\boldsymbol{x}}{||\boldsymbol{x}|| + \rho_3} - \rho_4 \,|\lfloor \boldsymbol{x} \rceil|^p \,, \tag{11}$$

with $\omega \in \mathcal{W}$, $\rho_1 > 0$, $\rho_2 > \delta_0$, $\rho_3 > 0$, and $\rho_4 \geq \delta_1$, then the solutions of the closed-loop system (10)-(11) *are uniformly predefined-time ultimately bounded with predefined bound. In fact, for any $T_c, b \in \mathbb{R}_+$, there exist some $\rho_1 > 0$, $\rho_2 > \delta_0$, $\rho_3 > 0$, and $\rho_4 \geq \delta_1$, such that the solutions $\boldsymbol{\Phi}_x(t, \boldsymbol{x}_0, t_0)$ of* (10) *satisfy $||\boldsymbol{\Phi}_x(t, \boldsymbol{x}_0, t_0)|| \leq b, \quad \forall t \geq t_0 + T_c$, with $\frac{\rho_3 \delta_0}{\delta_0 - \rho_2} = b$ and $\rho_1 = T_c$.*

Proof. Consider the Lyapunov function candidate $V(\boldsymbol{x}) = ||\boldsymbol{x}||$ and let $T_c, \mu \in \mathbb{R}_+$. The time-derivative of V along the solutions of the closed-loop system (10)-(11) satisfies

$$\begin{aligned}
\dot{V}(\boldsymbol{x}) &= |\lfloor \boldsymbol{x}^T \rceil|^0 \Bigg[-\frac{1}{\rho_1} \frac{||\lfloor \boldsymbol{x} \rceil||^0}{\omega'(||\boldsymbol{x}||)} - \rho_2 \frac{\boldsymbol{x}}{||\boldsymbol{x}|| + \rho_3} - \\
&\qquad \rho_4 \,|\lfloor \boldsymbol{x} \rceil|^p + \boldsymbol{\Delta}(t, \boldsymbol{y}) \Bigg] \\
&\leq -\frac{1}{\rho_1} \frac{1}{\omega'(V(\boldsymbol{x}))} - \rho_2 - \rho_2 \frac{\rho_3}{||\boldsymbol{x}|| + \rho_3} - \\
&\qquad \rho_4 ||\boldsymbol{x}||^p + ||\boldsymbol{\Delta}(t, \boldsymbol{y})|| \\
&\leq -\frac{1}{\rho_1} \frac{1}{\omega'(V(\boldsymbol{x}))} - \rho_2 - \rho_2 \frac{\rho_3}{||\boldsymbol{x}|| + \rho_3} - \\
&\qquad \rho_4 ||\boldsymbol{x}||^p + \delta_0 + \delta_1 ||\boldsymbol{x}||^p \\
&\leq -\frac{1}{\rho_1} \frac{1}{\omega'(V(\boldsymbol{x}))}, \quad \text{for } ||\boldsymbol{x}|| \geq \frac{\rho_3 \delta_0}{\delta_0 - \rho_2}.
\end{aligned}$$

This is, there exist $\rho_1 = T_c > 0$, and $\frac{\rho_3 \delta_0}{\delta_0 - \rho_2} = \mu$ such that $\dot{V}(\boldsymbol{x}) \leq -\frac{1}{T_c} \frac{1}{\omega'(V(\boldsymbol{x}))}$, for $||\boldsymbol{x}|| \geq \mu$. Hence, noticing that $V(\boldsymbol{x}) = \alpha(||\boldsymbol{x}||)$ with $\alpha(r) = r \in \mathcal{K}_\infty$ and using Theorem 1, the result follows. ☐

It is worth to notice that the parameters related to the predefined ultimate bound b, which are ρ_2 and ρ_3, are completely independent from the parameter related to the predefined convergence time T_c, which is ρ_1.

Remark 4. In controller (11), the term $\rho_2 \frac{\boldsymbol{x}}{||\boldsymbol{x}|| + \rho_3}$ mitigates the effect of the nonvanishing part of the disturbance, bounded by δ_0, whereas the term $\rho_4 \,|\lfloor \boldsymbol{x} \rceil|^p$ cancels the effect of the vanishing part of the disturbance, bounded by $\delta_1 ||\boldsymbol{x}||^p$. In this sense, both terms are relevant, but the second term is even more important because:

- in absence of the first term $\rho_2 \frac{\boldsymbol{x}}{||\boldsymbol{x}|| + \rho_3}$, the UPTUPB property would be lost, but at least the uniform ultimate boundedness property would be mantained, ensuring some robustness features;
- however, in absence of the second term $\rho_4 \,|\lfloor \boldsymbol{x} \rceil|^p$, the whole disturbance must be bounded, $\delta_0 + \delta_1 ||\boldsymbol{x}||^p \leq \bar{\delta}$, for the controller to maintain robustness properties. Nevertheless, one can see that for the state far from the origin the disturbance $\delta_0 + \delta_1 ||\boldsymbol{x}||^p$ may exceed any established bound $\bar{\delta}$.

C. Application scenarios

We consider two representative scenarios:

1) Case 1: $n = m$: In this case, the variable $\boldsymbol{x}$ can be selected as $\boldsymbol{x}(t, \boldsymbol{y}) = \boldsymbol{y} - \boldsymbol{y}_d(t)$. For this selection of $\boldsymbol{x}$, the control input (9) has the form

$$\boldsymbol{u} = -[\boldsymbol{B}(t, \boldsymbol{y})]^{-1} \Big[\boldsymbol{g}(t, \boldsymbol{y}) - \dot{\boldsymbol{y}}_d(t) - \boldsymbol{v} \Big]. \tag{12}$$

Hence, applying (12)-(11), the closed-loop solutions $\boldsymbol{\Phi}_y(t, \boldsymbol{y_0}, t_0)$ of system (6) comply to $||\boldsymbol{\Phi}_x(t, \boldsymbol{x_0}, t_0)|| = ||\boldsymbol{\Phi}_y(t, \boldsymbol{y_0}, t_0) - \boldsymbol{y}_d(t)|| \leq b$, for all $t \geq t_0 + T_c$. This is, the closed-loop solutions $\boldsymbol{\Phi}_y(t, \boldsymbol{y_0}, t_0)$ approximately tracks the desired reference function $\boldsymbol{y}_d : \mathbb{R}_{\geq 0} \to \mathbb{R}^n$ after the desired time T_c.

2) Case 2: $n = 2m$: In this case, we also assume that the functions $\boldsymbol{g}$ and $\boldsymbol{B}$ in affine control system (6) are

$$\boldsymbol{g}(t, \boldsymbol{y}) = \begin{bmatrix} \boldsymbol{y}_2 \\ \boldsymbol{g}_2(t, \boldsymbol{y}) \end{bmatrix} \text{ and } \boldsymbol{B}(t, \boldsymbol{y}) = \begin{bmatrix} \boldsymbol{0}_{m \times m} \\ \boldsymbol{B}_2(t, \boldsymbol{y}) \end{bmatrix},$$

such that system (6) has the particular form

$$\begin{aligned}
\dot{\boldsymbol{y}}_1 &= \boldsymbol{y}_2 \\
\dot{\boldsymbol{y}}_2 &= \boldsymbol{g}_2(t, \boldsymbol{y}) + \boldsymbol{B}_2(t, \boldsymbol{y})(\boldsymbol{u} + \boldsymbol{\delta}(t, \boldsymbol{y})),
\end{aligned} \tag{13}$$

where $\boldsymbol{y} = \begin{bmatrix} \boldsymbol{y}_1^T & \boldsymbol{y}_2^T \end{bmatrix}^T \in \mathbb{R}^n$, $\boldsymbol{y}_1, \boldsymbol{y}_2 \in \mathbb{R}^m$, $\boldsymbol{g}_2 : \mathbb{R}_{\geq 0} \times \mathbb{R}^n \to \mathbb{R}^m$, $\boldsymbol{B}_2 : \mathbb{R}_{\geq 0} \times \mathbb{R}^n \to \mathbb{R}^{m \times m}$ and $\boldsymbol{0}_{m \times m}$ is the $m \times m$ null matrix.

For this case, the variable $\boldsymbol{x}$ can be selected as

$$\boldsymbol{x}(t, \boldsymbol{y}) = \boldsymbol{y}_2 - \dot{\boldsymbol{y}}_{1,d}(t) + \rho_0 \left(\boldsymbol{y_1} - \boldsymbol{y}_{1,d}(t) \right), \tag{14}$$

with $\rho_0 > 0$ a parameter. For this selection of $\boldsymbol{x}$, the control input (9) has the form

$$\begin{aligned}
\boldsymbol{u} = -[\boldsymbol{B}_2(t, \boldsymbol{y})]^{-1} \Big[&\boldsymbol{g}_2(t, \boldsymbol{y}) - \ddot{\boldsymbol{y}}_{1,d}(t) + \\
&\rho_0 \left(\boldsymbol{y_2} - \dot{\boldsymbol{y}}_{1,d}(t) \right) - \boldsymbol{v} \Big].
\end{aligned} \tag{15}$$

Hence, applying (15)-(11), the closed-loop solutions $\boldsymbol{\Phi}_y(t,\boldsymbol{y_0},t_0) = \begin{bmatrix}\boldsymbol{\Phi}_{y1}(t,\boldsymbol{y_0},t_0)^T & \boldsymbol{\Phi}_{y2}(t,\boldsymbol{y_0},t_0)^T\end{bmatrix}^T$, with $\boldsymbol{\Phi}_{y1},\boldsymbol{\Phi}_{y2} \in \mathbb{R}^m$, of system (6) satisfy

$$\begin{aligned}||\boldsymbol{\Phi}_x(t,\boldsymbol{x_0},t_0)|| = \big|\big|\boldsymbol{\Phi}_{y2}(t,\boldsymbol{y_0},t_0) - \dot{\boldsymbol{y}}_{1,d}(t) + \\ \rho_0\Delta\boldsymbol{\Phi}_{y1}(t,\boldsymbol{y_0},t_0)\big|\big| \\ \leq b, \quad \forall t \geq t_0 + T_c,\end{aligned} \tag{16}$$

where $\Delta\boldsymbol{\Phi}_{y1}(t,\boldsymbol{y_0},t_0) = \boldsymbol{\Phi}_{y1}(t,\boldsymbol{y_0},t_0) - \boldsymbol{y}_{1,d}(t)$.

This behavior induces remarkable robustness properties, as stated and proved below.

Proposition 2 ([14]). *Considering property* (16)*, the following holds for the zero-state-response (i.e.,* $\Delta\boldsymbol{\Phi}_{y1}(t_0) = 0$*):*

$$||\Delta\boldsymbol{\Phi}_{y1}||_{L^2[t_0,t]} \leq \frac{\beta}{\rho_0} + \frac{b}{\rho_0}\sqrt{t - T_c}, \quad \forall t \geq t_0 + T_c,$$

where $||\Delta\boldsymbol{\Phi}_{y1}||_{L^2[t_0,t]} = \int_{t_0}^{t} ||\Delta\boldsymbol{\Phi}_{y1}(\tau,\boldsymbol{y_0},t_0)||\, d\tau$ *is the 2-Lebesgue norm of the vector function* $\Delta\boldsymbol{\Phi}_{y1}$ *and* $\beta > 0$ *is a finite constant.*

Proof. First note that $\boldsymbol{\Phi}_{y2} = \dot{\boldsymbol{\Phi}}_{y1}$, from (13). Hence, the solutions $\boldsymbol{\Phi}_x$ and $\boldsymbol{\Phi}_y$ of systems (10) and (6), respectively, are related as (see (14)) $\boldsymbol{\Phi}_x = \Delta\dot{\boldsymbol{\Phi}}_{y1} + \rho_0\Delta\boldsymbol{\Phi}_{y1}$.

To analyze the zero-state-response consider $\Delta\boldsymbol{\Phi}_{y1}(t_0) = 0$, and take Laplace transform at either sides of the above equation. This yields $\mathcal{L}\{\Delta\boldsymbol{\Phi}_{y1}\} = G(s)\mathcal{L}\{\boldsymbol{\Phi}_x\}$, with $G(s) = \frac{1}{s+\rho_0}$. Hence, using the Parseval Theorem for the system in steady-state ($s = jw$) [16], $||\Delta\boldsymbol{\Phi}_{y1}||_{L^2[t_0,t]} \leq ||G(\cdot)||_\infty ||\boldsymbol{\Phi}_x||_{L^2[t_0,t]}$, where $||G(\cdot)||_\infty = \sup_{w\in\mathbb{R}} |G(jw)| = \frac{1}{\rho_0}$. Consequently, for $t \geq T_c + t_0$ and using (16)

$$\begin{aligned}||\Delta\boldsymbol{\Phi}_{y1}||_{L^2[t_0,t]} &\leq \frac{1}{\rho_0}\left(\int_{t_0}^{t} ||\boldsymbol{\Phi}_x(\tau)||^2 \,\mathrm{d}\tau\right)^{1/2} \\ &\leq \frac{1}{\rho_0}\left(\int_{t_0}^{T_c} ||\boldsymbol{\Phi}_x(\tau)||^2 \,\mathrm{d}\tau\right)^{1/2} + \\ &\qquad \frac{1}{\rho_0}\left(\int_{T_c}^{t} b^2 d\varsigma\right)^{1/2} \\ &= \frac{\beta}{\rho_0} + \frac{b}{\rho_0}\sqrt{t - T_c}\end{aligned}$$

with $\beta := \left(\int_{t_0}^{T_c} ||\boldsymbol{\Phi}_x(\tau)||^2 \,\mathrm{d}\tau\right)^{1/2} > 0$ finite. □

Basically, Proposition 2 says that controller (13)-(11) induces finite-gain input-output stability of the tracking error $\Delta\boldsymbol{\Phi}_{y1}$ with respect to bounded disturbances, where the sensibility and performance of the tracking scheme can be tuned according to the system requirements and hardware capabilities, by means of the control parameters.

V. Simulation Example

Consider a planar, two-link manipulator with revolute joints as the one exposed in [18]. The longitudes and masses of the links are $l_1 = 0.15\,\mathrm{m}$, $l_2 = 0.07\,\mathrm{m}$, $m_1 = 1.5\,\mathrm{Kg}$ and $m_2 = 0.7\,\mathrm{Kg}$. The manipulator is operated in the plane, such that the gravity acts along the $z-$axis.

The model of the manipulator obtained via the Euler-Lagrange formalism is

$$\boldsymbol{H}(\boldsymbol{q})\ddot{\boldsymbol{q}} + \boldsymbol{C}(\boldsymbol{q},\dot{\boldsymbol{q}})\dot{\boldsymbol{q}} = \boldsymbol{\tau} + \boldsymbol{d}, \tag{17}$$

where $\boldsymbol{q},\dot{\boldsymbol{q}},\ddot{\boldsymbol{q}} \in \mathbb{R}^2$ are the (angular) position, (angular) velocity and (angular) acceleration in the joint space, $\boldsymbol{H}(\boldsymbol{q}) \in \mathbb{R}^{2\times 2}$ is the (symmetric positive definite) inertia matrix, $\boldsymbol{C}(\boldsymbol{q},\dot{\boldsymbol{q}}) \in \mathbb{R}^{2\times 2}$ is the Coriolis and centrifugal effects matrix, $\boldsymbol{\tau} \in \mathbb{R}^2$ is the vector of control inputs and $\boldsymbol{d} \in \mathbb{R}^2$ is a vector of unknown but bounded disturbances.

Defining $\boldsymbol{y}_1 = \boldsymbol{q}$, $\boldsymbol{y}_2 = \dot{\boldsymbol{q}}$ and $\boldsymbol{u} = \boldsymbol{\tau}$, the model (17) can be rewritten as (13), with $\boldsymbol{g_2}(t,\boldsymbol{y}) = -\boldsymbol{H}(\boldsymbol{y}_1)^{-1}\boldsymbol{C}(\boldsymbol{y}_1,\boldsymbol{y}_2)\boldsymbol{y}_2$, $\boldsymbol{B}_2(t,\boldsymbol{y}) = \boldsymbol{H}(\boldsymbol{y}_1)^{-1}$ and $\delta(t,\boldsymbol{y}) = \boldsymbol{d}$. With the numerical values in this example, $||\boldsymbol{B}_2(t,\boldsymbol{y})|| \leq 600$.

The purpose of this simulation example is to illustrate the behavior of the controller (15)-(11), with $\omega(r) = \frac{2}{\pi}\arctan(r^{1/2})$. To this end, the disturbance vector, caused by dry and viscous friction phenomena, has the form $\boldsymbol{d} = 0.2 + 0.1\sin(\dot{\boldsymbol{q}})$. Taking this into account, the term $\boldsymbol{\Delta}(t,\boldsymbol{y})$ is uniformly bounded by $||\boldsymbol{\Delta}(t,\boldsymbol{y})|| \leq \delta_0 + \delta_1||\boldsymbol{x}||$, with $\delta_0 = 0.2\times 600 = 120$ and $\delta_1 = 0.1\times 600 = 60$. The desired reference signal is $\boldsymbol{y}_d = \begin{bmatrix}\frac{\pi}{2}t - \pi & -\frac{\pi}{2}\end{bmatrix}^T$.

The solutions $\boldsymbol{\Phi}_x$ of system (10) must reach a vicinity of radius $b = 0.01$ of the origin in at most $T_c = 1\,\mathrm{s}$. Hence, the controller parameters are set to $\rho_0 = 10$, $\rho_1 = 1$, $\rho_2 = 240$, $\rho_3 = 0.01$, and $\rho_4 = 60$.

The simulations are conducted using the Euler integration method, with a time step size of 1×10^{-4}.

The performance of the two-link manipulator system (17) closed-loop by (15)-(11) is shown in Figs. 1-4. Fig. 1 shows that the solutions $\boldsymbol{\Phi}_x$ satisfy the UPTUPB property with the selected bound $b = 0.01$ and time $T_c = 1$. The tracking of the angular positions can be appreciated in Fig. 2, and the tracking in real world coordinates can be seen in Fig. 3. Finally, the continuous control torques are shown in Fig. 4.

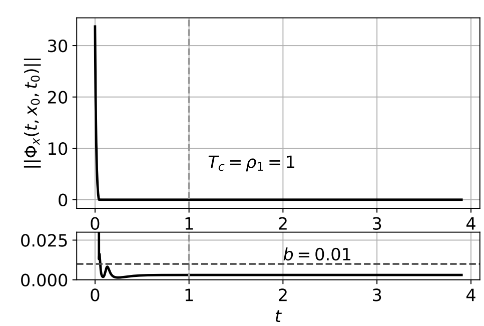

Fig. 1. Solutions $\boldsymbol{\Phi}_x$ of (10) for the two-link manipulator system. The UPTUPB property is satisfied.

VI. Conclusions

The design of a class of continuous predefined-time controllers was carried out in this paper. The *uniform predefined-time ultimate predefined boundedness* of the closed-loop

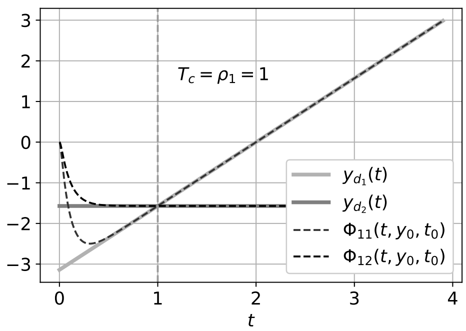

Fig. 2. Tracking of the joint angular positions.

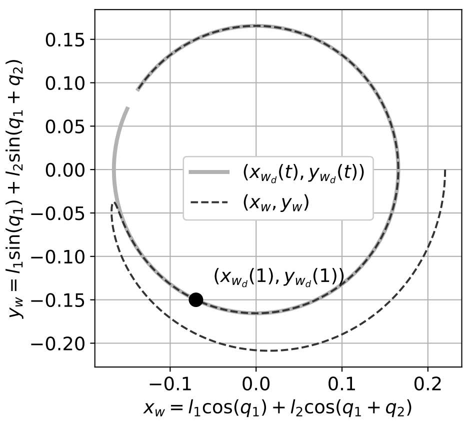

Fig. 3. Tracking in cartesian coordinates. The end effector follows a circumference with an approximate radius of $0.17\,\mathrm{m}$

solutions was demonstrated through a suitable Lyapunov-like framework, which was also studied in this document. It was also shown that for a class of second-order systems, the finite-gain input-output stability property is achieved by the proposed controller. Finally, all the mentioned features were highlighted through a representative numerical simulation example.

ACKNOWLEDGMENT

Esteban Jiménez acknowledges to CONACyT, México for the DSc scholarship number 481467.

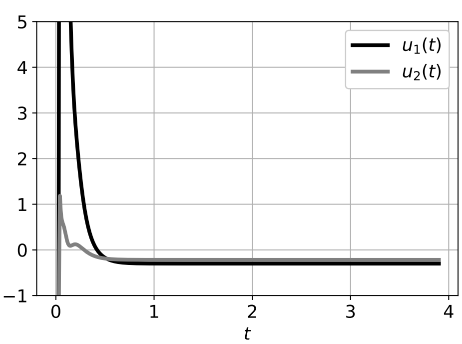

Fig. 4. Continuous control torques.

REFERENCES

[1] E. Roxin, “On finite stability in control systems,” *Rendiconti del Circolo Matematico di Palermo*, vol. 15, no. 3, pp. 273–282, 1966.

[2] V. Haimo, “Finite time controllers,” *SIAM Journal on Control and Optimization*, vol. 24, no. 4, pp. 760–770, 1986.

[3] S. Bhat and D. Bernstein, “Finite-time stability of continuous autonomous systems,” *SIAM Journal on Control and Optimization*, vol. 38, no. 3, pp. 751–766, 2000.

[4] E. Moulay and W. Perruquetti, “Finite time stability conditions for non-autonomous continuous systems,” *International Journal of Control*, vol. 81, no. 5, pp. 797–803, 2008.

[5] V. Andrieu, L. Praly, and A. Astolfi, “Homogeneous approximation, recursive observer design, and output feedback,” *SIAM Journal on Control and Optimization*, vol. 47, no. 4, pp. 1814–1850, 2008.

[6] E. Cruz-Zavala, J. Moreno, and L. Fridman, “Uniform second-order sliding mode observer for mechanical systems,” in *Variable Structure Systems (VSS), 2010 11th International Workshop on*, june 2010, pp. 14 –19.

[7] A. Polyakov, “Nonlinear feedback design for fixed-time stabilization of linear control systems,” *IEEE Transactions on Automatic Control*, vol. 57, no. 8, pp. 2106–2110, 2012.

[8] A. Polyakov and L. Fridman, “Stability notions and lyapunov functions for sliding mode control systems,” *Journal of the Franklin Institute*, vol. 351, no. 4, pp. 1831 – 1865, 2014, special Issue on 2010-2012 Advances in Variable Structure Systems and Sliding Mode Algorithms.

[9] J. D. Sánchez-Torres, D. Gómez-Gutiérrez, E. López, and A. G. Loukianov, “A class of predefined-time stable dynamical systems,” *IMA Journal of Mathematical Control and Information*, vol. 35, no. Suppl 1, pp. i1–i29, 2018.

[10] E. Jiménez-Rodríguez, J. D. Sánchez-Torres, and A. G. Loukianov, “On optimal predefined-time stabilization,” *International Journal of Robust and Nonlinear Control*, vol. 27, no. 17, pp. 3620–3642, 2017, rnc.3757. [Online]. Available: http://dx.doi.org/10.1002/rnc.3757

[11] J. D. Sánchez-Torres, M. Defoort, and A. J. Muñoz-Vázquez, “A second order sliding mode controller with predefined-time convergence,” in *2018 15th International Conference on Electrical Engineering, Computing Science and Automatic Control (CCE)*, Sept 2018.

[12] E. Jiménez-Rodríguez, J. D. Sánchez-Torres, D. Gómez-Gutiérrez, and A. G. Loukianov, “Variable structure predefined-time stabilization of second-order systems,” *Asian Journal of Control*, vol. 21, no. 3, pp. 1179–1188, May 2019.

[13] J. D. Sánchez-Torres, M. Defoort, and A. J. Muñoz-Vázquez, “Predefined-time stabilisation of a class of nonholonomic systems,” *International Journal of Control*, pp. 1–8, 2019.

[14] A. J. Muñoz-Vázquez, J. D. Sánchez-Torres, E. Jiménez-Rodríguez, and A. Loukianov, “Predefined-time robust stabilization of robotic manipulators,” *IEEE/ASME Transactions on Mechatronics*, pp. 1–1, 2019.

[15] A. J. Muñoz-Vázquez, J. D. Sánchez-Torres, S. Gutiérrez-Alcalá, E. Jiménez-Rodríguez, and A. G. Loukianov, “Predefined-time robust contour tracking of robotic manipulators,” *Journal of the Franklin Institute*, vol. 356, no. 5, pp. 2709 – 2722, 2019.

[16] H. Khalil, *Nonlinear Systems*, ser. Pearson Education. Prentice Hall, 2002.

[17] C. M. Kellett, “A compendium of comparison function results,” *Mathematics of Control, Signals, and Systems*, vol. 26, no. 3, pp. 339–374, Sep 2014.

[18] V. I. Utkin, J. Guldner, and J. Shi, *Sliding Mode Control in Electro-Mechanical Systems, Second Edition (Automation and Control Engineering)*, 2nd ed. CRC Press, 5 2009.